

Measurements of depletion layers in hydrogenated amorphous silicon

R. A. Street

Xerox Palo Alto Research Center, 3333 Coyote Hill Road, Palo Alto, California 94304

(Received 22 December 1982)

The use of transient photoconductivity for measuring and profiling the depletion-layer electric field in amorphous silicon is described. Charge-collection measurements yield the depletion-layer width, and this technique is used to study various sample structures. The internal-field profile is obtained from the transient photocurrent response. We report measurements on Cr, Pd, and Pt contacts and obtain the built-in potentials and density-of-states data.

I. INTRODUCTION

The band bending at the surface of hydrogenated amorphous silicon (a -Si:H) films is important for several reasons. First, because the samples are thin films, the depletion layer often dominates measurements of bulk properties such as dc conductivity.¹ Second, in view of recent investigations of Schottky barriers on a -Si:H,²⁻⁴ measurements of the built-in potential and the depletion profile are of interest. Third, and perhaps most important, the energy distribution of gap states, $N(E)$, is usually deduced from studies involving the depletion layer.

The most common techniques applied to studies of the depletion layer are the field effect⁵ and various capacitance measurements,⁶ including deep-level transient spectroscopy (DLTS).⁷ These are standard techniques for crystalline semiconductors, but each has some problems in their application to amorphous semiconductors. For example, the field effect is sensitive to surface states, and the accuracy with which structure in $N(E)$ can be obtained has been questioned.¹ The problem with capacitance techniques is the low conductivity of undoped a -Si:H. The measurements must be made at low frequency to access all the states and often can only be made on doped a -Si:H whose density of states is known to be different from that of undoped a -Si:H.

This paper describes how transient photoconductivity can be used to measure the electric field profile of a depletion layer. The measurement is simple and direct and is particularly applicable to low-conductivity and low-mobility materials such as a -Si:H. The technique is the same as is widely used in time-of-flight (TOF) drift-mobility measurements so that the validity of the experiment is well established. The TOF experiment measures the drift mobility through the response of the carriers to a known applied field. It is obvious that if the mobility is known, then the observed response can be used to obtain the field distribution under which the carriers

move. This idea can be applied in various ways. One method used by Datta and Silver⁸ is to vary the excitation wavelength and apply a reverse field to obtain an average depletion-layer field. An alternative method is to use charge-collection measurements, and this has been applied to solar cells by Spear *et al.*⁹ Our experiments use the charge-collection method and also obtain the internal-field profile directly from the transient response.

Section II outlines the use of the TOF experiments for measuring depletion layers and for general characterization of sample. Section III discusses the qualitative effects that can be observed in various sample structures, and then gives a more quantitative analysis of different Schottky-barrier contacts.

II. MEASUREMENT DETAILS

A. Samples

The samples are all undoped a -Si:H deposited by plasma decomposition of SiH_4 as described elsewhere.¹⁰ Samples were typically 4–7 μm thick with semitransparent electrodes of Cr, Pd, or Pt on each side. In some samples the bottom contact also had a 400-Å-thick n^+ a -Si:H layer. Measurements on samples with evaporated bottom contacts usually exhibited distortion of the transient for times up to ~ 20 nsec due to the RC time constant. For the more quantitative measurements in Sec. III C, samples were deposited on Al substrates, which gave a faster response.

The excitation used 7-nsec pulses from a nitrogen pulsed-dye laser at approximately 5500 Å, at which wavelength the absorption depth is ~ 1500 Å. The pulses were usually separated by 10 sec to ensure that the sample remained close to its equilibrium state, and typically up to 10 pulses were averaged for a single transient. The photocurrent was measured by a transient digitizer at 5-nsec intervals. The total charge collected was no greater than 10^{-11} C per pulse, which was low enough to avoid space-

charge effects. This charge corresponds to a field drop of $\sim 10^2$ V/cm for a typical sample.

B. Measurements

Three different measurement techniques were used as follows.

(a) *Pulsed field transient.* In the standard TOF experiment, the voltage is applied shortly before the light pulse. This is essential if a uniform electric field is required, because a dc applied voltage will usually be dropped across one or other electrode (see below). To prevent distortion of the field, the interval between the voltage and light pulse must be less than the dielectric relaxation time. In our experience, this time is of order 1 sec for undoped *a*-Si:H. We confirmed that the response was independent of delay times up to at least 1 msec and typically used 50 μ sec. It should be noted that the field applied in this way adds directly to any internal field.

The photocurrent J resulting from the applied field F is

$$J = \eta n e \mu F, \quad (1)$$

where n is the number of photons absorbed, η is the carrier generation efficiency, and μ is the drift mobility of the carrier selected for transport by the polarity of the applied field. The mobility is obtained from the transit time τ_T ,

$$\mu = d / F \tau_T, \quad (2)$$

where d is the sample thickness. For nondispersive transport, τ_T is defined as the time at which J drops by 50%, while for dispersive transport it is given as usual by the change of slope in a $\log J$ - $\log t$ plot.

(b) *dc field transient.* If a constant voltage is applied for more than about 1 sec, the field in the sample becomes nonuniform and typically is confined to the depletion layer of one of the electrodes. In particular, if no voltage is applied to the sample, the internal field will be that corresponding to the type of contact made to the sample. For example, metals such as Pt and Pd are known to form Schottky contacts with an electron depletion layer. On the other hand, an n^+ contact should form a barrier to holes. The main aim of the paper is to show that the TOF experiment is an excellent probe of how the internal field is distributed in a sample. The photoexcited carrier will of course move under the action of the internal field, and the transient photocurrent is therefore a direct measure of the field.

The depletion field F depends on the distance x into the sample, so that the photocurrent is time dependent, corresponding to the drift of the charge packet down the field,

$$J(t) = \eta n e \mu F(t). \quad (3)$$

For carriers that start at $x=0$ at time $t=0$, x is related to t by

$$x = \int_0^t \mu F(t') dt'. \quad (4)$$

$F(x)$ can therefore be obtained directly from measurement of $J(t)$ using Eq. (4), provided that $F(t)$ and the mobility are known. Since the current is proportional to the field, $F(t)$ can be found by comparing the current to that obtained for a known applied field and using Eq. (1) as in the TOF experiment. In this way, the number of carriers ηn does not need to be known, provided it is the same for the two experiments. This point is discussed in Sec. III C.

(c) *Charge collection.* The charge collection (equal to $\int J dt$) is a direct and convenient measure of the average distance moved by the carriers before deep trapping occurs. When a uniform electric field is applied and there is a single deep trapping lifetime τ_D , then the charge collection Q is given by

$$Q = \eta n (\mu \tau_D F / d) [1 - \exp(-d / \mu \tau_D F)]. \quad (5)$$

$Q=1$ (in units of ηn) corresponds to complete transit of all the carriers. When $Q \lesssim 0.5$, the exponential term is negligible so that

$$Q = x / d, \quad (6)$$

where $x = \mu \tau_D F$ is the carrier range. When the field is nonuniform, Eq. (6) remains valid as a measure of the range x although, of course, now x is no longer simply related to $\mu \tau_D$.

If the nonuniform field is that of the depletion layer, then the range will measure the depletion width provided τ_D is large enough. The carriers move rapidly down the depletion field until they reach the field-free region. At this point further motion is determined by diffusion rather than drift. Diffusion lengths in *a*-Si:H tend to be small, and in any event there is no net direction associated with the diffusion. Therefore, to a good approximation the carriers stop at the end of the depletion layer, and this distance is measured by the charge collection. In practice we use charge-collection measurements to provide a qualitative probe of the internal field, and the transient response for more detailed investigations.

C. The generation efficiency

The generation efficiency η is a parameter which determines the total charge collected. Provided that η is constant, its absolute value is immaterial because Q is always scaled to its saturation value at full collection. However, a field dependence of η could have a major effect on the results. Mort *et al.*¹¹ have reported a field dependence above

3×10^4 V/cm as η increases from ~ 0.5 to unity. Other reports find no change at all in η . Our measurements are all below about 5×10^4 V/cm, and so a constant η is a valid approximation. In addition, the next section describes further evidence that η is indeed constant in our samples.

III. RESULTS AND DISCUSSION

A. Pulsed field measurements

Figure 1 shows time-of-flight data for electrons in *a*-Si:H for several different uniform applied fields including $F=0$. Illumination is through a semitransparent Cr electrode. At high fields a normal transit is observed with a drift mobility μ_E of about 2.5 $\text{cm}^2/\text{V sec}$, which is the largest value we have observed at room temperature in *a*-Si:H and compares with other reports of μ_E of about 1 $\text{cm}^2/\text{V sec}$.¹² The electron transport is nondispersive, but has substantial Gaussian rounding at the end of the pulse, in general agreement with other measurements.¹² At zero applied field, an electron response is still observed due to motion of the electrons in the internal field of the depletion layer. The initial photocurrent, compared to that under an applied field, indicates that the field near the surface is 10^3 V/cm or

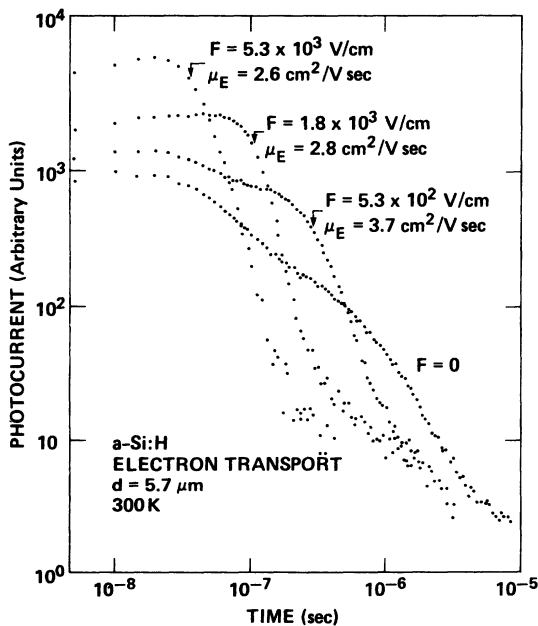


FIG. 1. Electron-transport measurements at different applied fields as indicated. The vertical scale is the same for each transient. The transit times are indicated by arrows and are used to obtain the drift mobility. The response at zero applied field is due to electrons drifting down the internal field.

more. Measurements to profile the internal field are described in more detail in Sec. III C. At intermediate applied fields, the transient is distorted by the internal field. This effect can be clearly seen in Fig. 1 for the response at 5.3×10^2 V/cm and can result in errors in calculating the mobility. For example, at this field the mobility appears to be 3.7 $\text{cm}^2/\text{V sec}$. The reason for this high value is that the internal field is much larger than the applied field for a substantial fraction of the sample.

Figure 2 shows equivalent data for hole transport. For these experiments the illumination was through an n^+ contact. Holes are observed to be dispersive with parameter $\alpha \sim 0.7$ at room temperature. The hole mobility is 1.2×10^{-2} $\text{cm}^2/\text{V sec}$ for an applied field of 5×10^4 V/cm, and obeys the expected field dependence of $F^{1/\alpha-1}$ as predicted by theories of dispersive transport. As for electrons, there is a hole response at zero field, which distorts the hole transit at all applied fields. This effect is again due to the depletion field. However, part of the response, particularly at short times, may also be due to electrons moving towards the illuminated contact. Although the total contribution to the charge collection from these carriers is very small, the higher mobility of the electrons can make them dominate the photocurrent at short times.

Figure 3 is a typical example of charge-collection data for electrons, which also shows an interesting phenomenon. The sample has no n^+ layer and is sandwiched between identical Cr contacts. The two sets of data correspond to illumination through each electrode, and the results show a very different

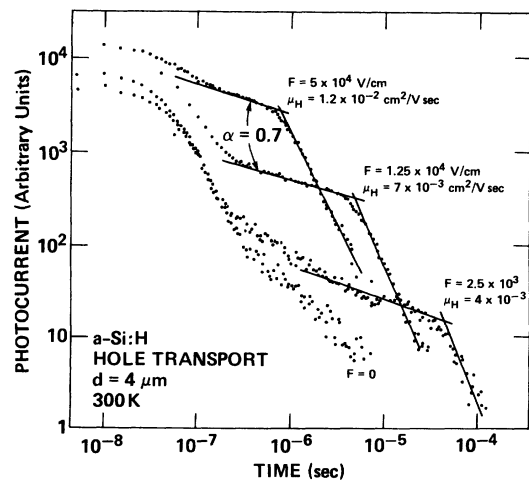


FIG. 2. Hole-transport measurements showing dispersive mobility with $\alpha \approx 0.7$. The response of the depletion-layer field shows in all the transients at times less than 10^{-7} sec.

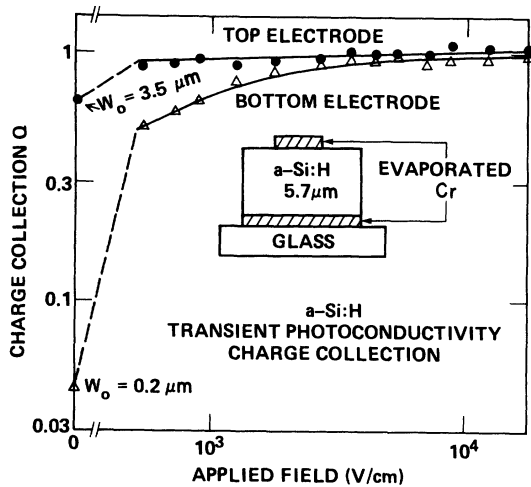


FIG. 3. Charge-collection data at different pulsed applied fields of both electrodes for the sample structure as shown. The top contact has a depletion width of $3.5 \mu\text{m}$ and the bottom contact only $0.2 \mu\text{m}$

behavior. Through the top electrode there is only about 10% decrease in charge collection for fields down to $5 \times 10^2 \text{ V/cm}$. Even at zero applied field Q is ~ 0.6 , which corresponds to a depletion width of $3.5 \mu\text{m}$. The wide depletion layer makes it hard to apply the Hecht analysis [Eq. (5)] because the internal field is not uniform. However, it is evident that the value of $(\mu\tau_D)_E$ is at least $10^{-6} \text{ cm}^2/\text{V}$. The flat response also implies that any changes in the photogeneration efficiency η is less than 10% for the observed range of applied field. This result does not necessarily mean that the photogeneration is independent of field, because the depletion layer ensures that the field in the generation region actually varies very little in all these experiments (see Sec. III C). However, it means that in practice η can be assumed constant to good accuracy. We note that any attempt to measure the field dependence of η must take into account the internal field which is typically 10^3 – 10^4 V/cm near a metal contact.

The results for the bottom contact shown in Fig. 3 are very different. First, the zero-field collection is only ~ 0.04 , indicating a depletion width of $\sim 0.2 \mu\text{m}$. Second, Q decreases substantially below $3 \times 10^3 \text{ V/cm}$. The first result clearly indicates that the two contacts are very different so that the properties of the interface are sensitive to the order of deposition. The most obvious explanation is that the initial deposition of *a*-Si:H yields material with a high defect density so that the Schottky barrier is screened out over a short distance. Other measurements particularly on sputtered *a*-Si:H have also found that the initial layer is defective.¹³

The obvious interpretation of the reduction of Q at weak fields is also that there are defects near the bottom contact. However, the analysis is again complicated by the wide depletion layer of the top contact. The electrons now must move against this depletion field, so that a complete transit is impossible at low applied fields. It is unclear whether this effect completely accounts for the reduction in Q . However, the results illustrate the point that the Hecht analysis becomes inaccurate when the depletion layer is more than about 20% of the sample thickness.

B. dc bias measurements

Figure 4 shows charge-collection data for the same sample as in Fig. 3, but in this case for a dc applied field. Again, illumination is through either contact, and the polarity of the voltage in Fig. 4 is with respect to the illuminated contact. For the analysis of this experiment, the sample can be considered as a pair of back-to-back Schottky barriers. When either Cr contact is in reverse bias, Q increases until it reaches ~ 1 , showing that full depletion of the sample can be achieved. In forward bias Q is approximately zero, confirming that the voltage is indeed all dropped across the reverse biased Schottky barrier.

To demonstrate that the pulsed and dc fields do indeed measure different properties, Fig. 5 shows the photocurrent transients for the two cases. The

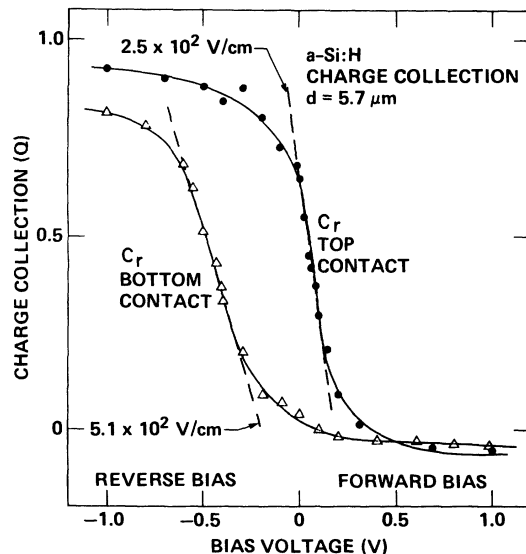


FIG. 4. Charge-collection data for varying dc bias in the same sample as in Fig. 3, again showing the different response of the top and bottom contacts. $Q > 0$ ($Q < 0$) gives the regime of electron (hole) transport.

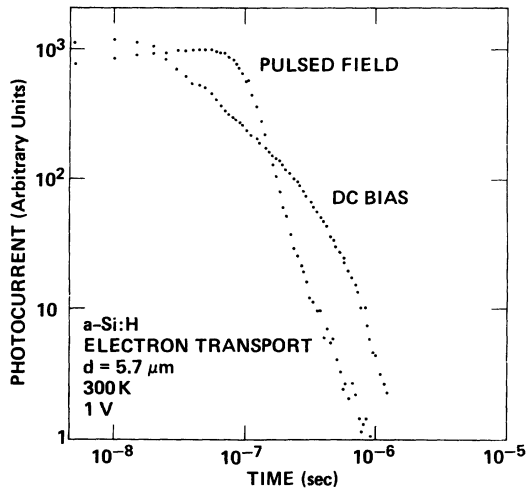


FIG. 5. Examples of the transient response for a pulsed applied field and a dc bias. The absence of a clear transit time for dc bias is because the internal field is nonuniform.

pulsed field gives a flat response with an abrupt turnoff, corresponding to the electron transit. The dc response decreases monotonically corresponding to the electrons moving down the nonuniform, decreasing field of the depletion layer.

In Fig. 4 the asymmetry of the two Cr contacts observed in Fig. 3 is again seen. The depletion layer at the top remains up to ~ 0.2 V of forward bias, which corresponds approximately to the built-in potential. On the other hand, the bottom depletion layer does not build up until an equivalent 0.2 V of reverse bias. This offset corresponds to a difference in effective barrier height, which (in Sec. III A) we ascribe to surface states. The offset also accounts for the photovoltage of 0.24 V measured for this sample.

The data in Fig. 4 is analogous to capacitance-voltage measurements, since capacitance, like charge collection, measures the depletion-layer width. In principle the density of states could be derived from the data, just as for C - V measurements. We have not attempted this analysis, but note that the quantity dV/dW_0 , where W_0 is the depletion width, should give the electric field at the surface. This quantity is given in Fig. 4 for the linear region near $Q=0.4$. The field at the top surface is found to be about half that at the bottom, again indicating a larger density of states near the bottom electrode.

Figure 6 shows similar Q - V data, but for a sample which had an n^+ bottom contact. A different response is expected for this sample because the n^+ layer forms a hole depletion layer, unlike the metal contacts. Comparison with Fig. 4 shows immediate-

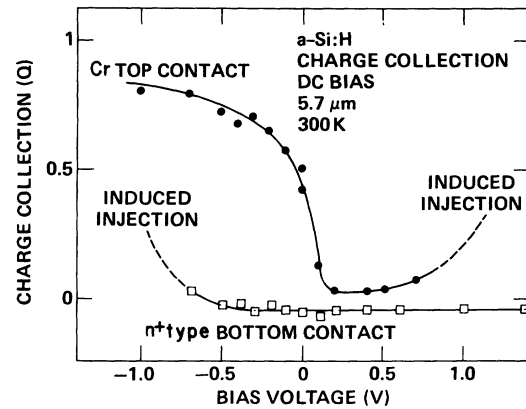


FIG. 6. Charge-collection data for varying dc bias on a sample with an n^+ back contact.

ly that the contact properties are indeed different. When the Cr top contact is in reverse bias, the depletion width again builds up until the sample is essentially fully depleted. None of the potential is dropped across the n^+ contact, even though it is also in reverse bias as a hole barrier, which confirms the usual assumption for this type of contact.

In forward bias, the response to the light pulse changes completely and in an interesting way. A typical transient is shown in Fig. 7. The response now extends for up to 1 sec instead of $\sim 1 \mu\text{sec}$ as in Figs. 1, 2, and 5. In addition, the charge collection Q is 2×10^4 . Clearly a conventional transit is not being observed here. Since the sample is in forward bias, it is possible that photoconductive gain is being observed, but this would imply an electron or hole lifetime of ~ 1 sec, whereas from the measured $\mu\tau_D$, the actual lifetime of either carrier does not exceed

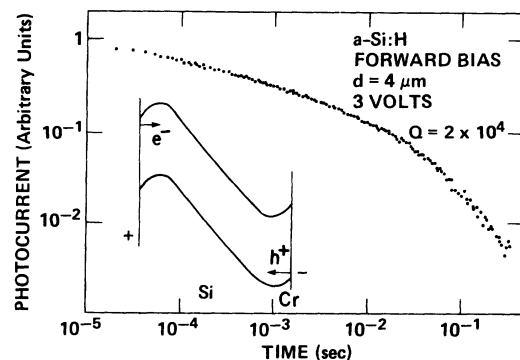


FIG. 7. Transient photoconductivity response under conditions of forward bias. Note the long response time and the very large charge collection. The inset shows the expected band diagram in forward bias.

10^{-5} sec. Instead, we interpret the result as a modification of the injection properties of the contact. Our model to explain the results is as follows. In forward bias, the band diagram is as shown in Fig. 7. The reversal of the field at one or both of the contacts is due to series resistance and leads to a potential well for electrons near the Cr contact and for holes near the n^+ contact. We suggest that the photogenerated electrons and holes will move into one or other of these potential wells and so change the space-charge distribution. This in turn increases the injection and so increases the measured current. After the light pulse the sample returns to equilibrium through recombination at the potential well. However, in the region of the well for holes, electrons tend to be excluded (and vice versa), so that the recombination rate can be very small, even under conditions of moderately large forward current.

This anomalous response in forward bias is probably the same as that observed by Datta and Silver,¹⁴ who suggested that space-charge relaxation was responsible. However, this mechanism could not explain the large value of Q observed here.

Figures 4 and 6 show that under reverse bias the samples become fully depleted. This effect can be observed directly by measuring the hole response from the back contact, and some examples are shown in Fig. 8. At zero bias the hole response is indicative of the hole depletion layer due to the n^+ contact which has width $\sim 0.3 \mu\text{m}$. Figure 6

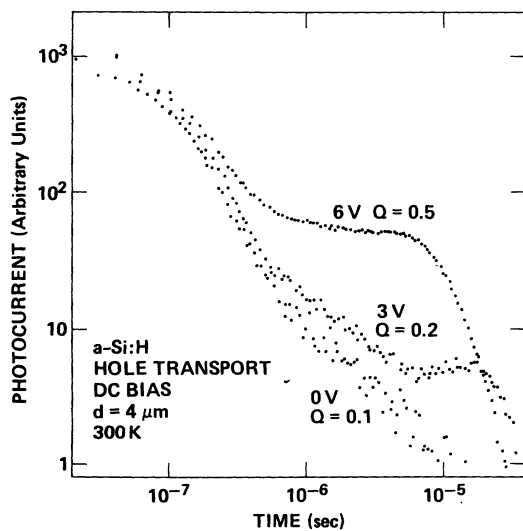


FIG. 8. Hole transport from the illuminated n^+ contact when the Cr electrode is in reverse bias. When the sample is fully depleted, the internal field extends to the n^+ contact so that holes can make the complete transit.

shows that when the Cr contact is under reverse bias, the response of the n^+ contact is unchanged, showing that the voltage is all dropped across the Cr electrode. However, when the bias is increased above 2 V the response of the n^+ contact does change. For example, under 3 V reverse bias (n^+ contact positive) most of the transient is the same except near 10^{-5} sec when the current first increases before dropping rapidly. This is a result of the onset of full depletion. The holes move down the n^+ barrier, move slowly through the low-field region where the two depletion layer just meet, then finally get accelerated as they move into the increasing field of the Cr depletion layer. It is the increasing field that causes the rise in photocurrent. At 6 V of bias the two depletion layers overlap quite strongly and a large enhancement of the current is seen. The increase in photocurrent expected in this experiment tends to be offset by the dispersive nature of the hole transport in which the mobility decreases with time. The combination of these two effects explains the flat response at 6 V.

C. Depletion-layer profiles

The measurements described above are aimed at a qualitative understanding of the depletion layers. This section discusses a more quantitative analysis. The main interest in having an accurate profile of the internal field is that the density of states can then be readily obtained.

Figures 9 and 10 show some results for the depletion layers of *a*-Si:H with Pt and Cr electrodes evaporated onto the same samples. Figure 11 shows similar data for Pd electrodes on two different samples which had larger defect densities. In each case the substrate was Al, which gave a faster response at short times than the evaporated back contact, and therefore a more accurate profile. The electron mobility was measured with an appropriate applied field which ensured full collection, and the internal field was obtained by scaling the photocurrent to that observed during the transit under the known applied field. The position of the charge packet was calculated using Eq. (4) to obtain the profiles shown in Figs. 9 and 11. Also shown in Figs. 10 and 11 are the potential profiles obtained by integrating the field.

Before describing the results in more detail, it is useful to outline the possible sources of error in these measurements. The main source of inaccuracy in the transient photocurrent experiments arises from the limited time resolution. Within our minimum timing period (5 nsec), electrons at the top of the depletion layer move $\sim 2000 \text{ \AA}$. An accurate

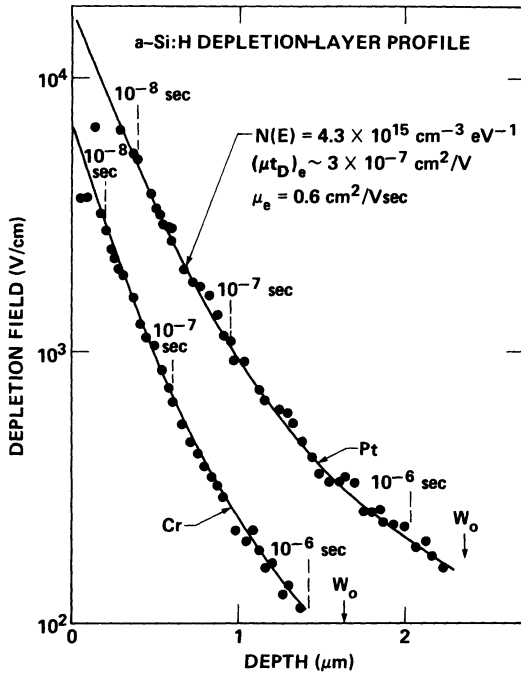


FIG. 9. Examples of the internal-field profile for Cr and Pt contacts to the same sample. The times marked correspond to those of the transient response. The values of W_0 are obtained from charge-collection measurements. $N(E)$ is derived from the exponential region of the field profile.

profile, therefore, really requires a time resolution ~ 1 nsec or better. However, a simple trick to improve the resolution is to apply a retarding field. A low positive bias is applied shortly before the excita-

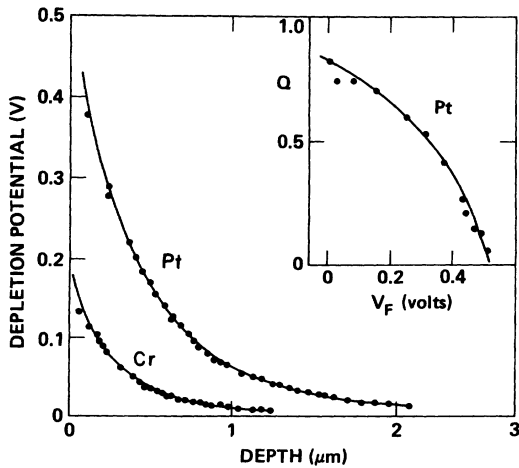


FIG. 10. Measurement of the depletion potential obtained by integrating the field profiles in Fig. 9. The inset shows charge collection for a Pt contact in forward bias, showing the collapse of the depletion layer at 0.5 V.

tion pulse. This gives a known uniform field (as in the TOF experiment), which subtracts from the depletion field. If this field is not too large, electrons are still drawn into the sample, but with lower velocity and therefore improved spatial resolution. The data in Figs. 9 and 11 use several different retarding fields to improve the accuracy of $F(x)$ at small x .

Second is the intrinsic spatial resolution. The absorption depth cannot be reduced much below 500 Å without losing many carriers to surface recombination. There is also a tendency for the drifting carrier packet to spread out as in the TOF experiment. Extreme dispersive transport would probably invalidate the present simple analysis. Fortunately, electrons in *a*-Si:H are not dispersive at room temperature. In addition, because the electrons move towards a decreasing field, those further forward move slower, and there is a natural tendency for the charge packet to close up. Providing the depletion width is at least 1000–2000 Å, the width of the charge packet does not seem to be a major problem.

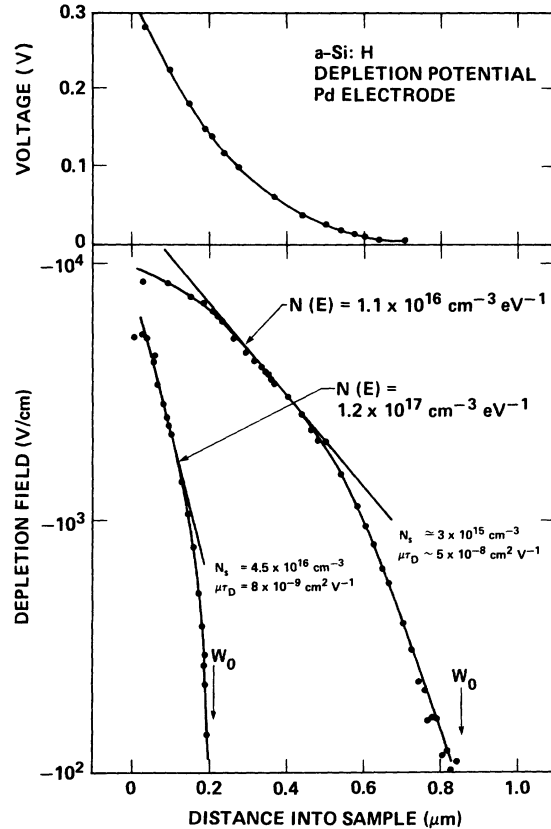


FIG. 11. Similar measurements of the field and potential profiles for two samples with higher defect density and Pd electrodes. The values of N_s are obtained from ESR measurements.

A third source of error is deep trapping of the charge, which results in the measured field being below the true value. For each sample, we have measured $\mu\tau_D$ for electrons from charge-collection data, and so can obtain the average deep trapping times. For the sample in Fig. 9, $\tau_D \sim 5 \times 10^{-7}$ sec. The measurement times are indicated in Fig. 9, from which it is clear that most of the depletion layer is covered within τ_D . The data in Fig. 11 corresponds to samples with much smaller $\mu\tau_D$, so the available time is reduced. In these samples the field tends to be larger because the depletion width is reduced, so that most of the layer can still be profiled. However, a comparison of the results shows a strong decrease in $F(x)$ at large x in samples of low $\mu\tau_D$, but not in the sample with the largest $\mu\tau_D$. This decrease almost certainly corresponds to the onset of deep trapping which restricts the measurable part of the layer.

Finally, the experiments assume that the charge density n in Eqs. (1) and (3) is constant. A field dependence of n introduces an error in the determination of $F(0)$, and this in turn introduces a scaling factor in both $F(x)$ and x . The fact that consistent measurements are obtained with different retarding fields leads us to deduce that n is in fact constant, and the data of Fig. 3 also led to the same conclusion.

From the above discussion we conclude that the technique provides a quantitative measurement of $F(x)$ except at distances less than 0.1–0.2 μm and at times larger than the deep trapping time. The first problem can be solved by better time resolution (~ 1 nsec should be adequate), and if the distribution of deep trapping times is known, a correction to the data could resolve the second point. At present we have not made either improvement. In view of this, it is inappropriate to use the data for a complete analysis of the density of states. Instead, we note that an exponential decrease in $F(x)$ corresponds to a uniform distribution of states, and this gives a reasonable fit to the data over the middle region where it is most accurate. In each case, the values of $N(E)$ deduced from the slope are shown in Figs. 9 and 11. The data in Fig. 9, which are least affected by deep trapping, show that $N(E)$ probably increases slowly away from the Fermi energy. The measurements in fact correspond to values of $N(E)$ at energies 0.1–0.3 eV below the bulk Fermi energy.

The dangling-bond densities N_s are known for the samples in Fig. 11 from ESR measurements. Based on the measured value of $\mu\tau_D N_s$ of $3.5 \times 10^8 \text{ cm}^{-1} \text{ V}^{-1}$ for dangling bonds,¹⁵ we deduce that for the sample of Fig. 10, $N_s \approx 1 \times 10^{15} \text{ cm}^{-3}$. In each case, therefore, $N(E)$ (measured in $\text{cm}^{-3} \text{ eV}^{-1}$) is 3–4 times larger than N_s (cm^{-3}). The data there-

fore indicate a defect band which is 0.25–0.35 eV wide, and located at or just below E_F . This result is as anticipated for the dangling bonds and is also substantially in agreement with DLTS measurements on doped samples.⁷

The measurements of the built-in potential V_B give values ~ 0.2 V for Cr, ~ 0.3 V for Pd, and ~ 0.5 V for Pt. At present the accuracy is probably only ± 0.05 V, because the potential varies strongly in the first 2000 Å, which is the region of greatest uncertainty in $F(x)$. In Figs. 4 and 6, it was found that the Cr depletion layer dropped to zero at ~ 0.2 V of forward bias, which is consistent with these results. The inset in Fig. 10 shows similar data for a 2- μm -thick sample with a Pt contact. From this a value for V_B of 0.5 V is found, in good agreement with the profiling data.

Previous electrical measurements find a barrier height of 0.97 V for Pd and 1.2 V for Pt on our samples,⁴ and other groups have reported similar values.³ The difference of 0.2 V is in good agreement with our measurements and implies that the Fermi energy is 0.7 V below the conduction band, again in reasonable agreement with other data. The built-in potential for Cr implies a barrier height of 0.9 V. Measurements of internal photoemission have found a value of 0.83 eV.³ These results therefore confirm that the field profiles deduced from these TOF experiments are accurate.

IV. CONCLUSIONS

These measurements are the first detailed study of Schottky-barrier depletion layers using transient photoconductivity. The technique is a simple and convenient way of investigating the internal field of any electrical contact. It is also the only method of obtaining the field profile without changing the applied bias. The evaluation of the built-in potential and the comparison with the depletion-layer width found by charge collection show that the field profile is accurate to within 10–20% over most of the depletion layer. Further improvement in the experimental technique should increase the accuracy and allow the density-of-states distribution to be obtained.

Charge-collection measurements provide an alternative measurement of the depletion width, which is particularly useful for qualitative measurements of electrical contacts. Again with further refinements of the experiment, it should be possible to obtain the density of states from data such as in Fig. 4.

The transient photoconductivity method offers advantages over the alternative techniques for measuring $N(E)$. First, because the field is profiled

throughout the depletion layer, surface states do not enter into the analysis. Second, long dielectric relaxation times do not present a problem. Instead, these are required by the experiment. Capacitance measurements, on the other hand, require that the space charge responds to the ac field so that experiments on undoped a -Si:H must be done at extremely low frequency. For this reason, capacitance DLTS has only been reported on doped a -Si:H. However, $N(E)$ is known to change with doping, so that the results are not applicable to undoped material. The

techniques described here should prove to be more suitable and more accurate for undoped a -Si:H.

ACKNOWLEDGMENTS

The author is grateful to R. Lujan and J. Zesch for sample preparation and to N. Johnson, R. Nemanich, and M. Thompson for helpful discussions. This research is supported by the Solar Energy Research Institute on Contract No. XB-2-02105-1.

-
- ¹H. Fritzsche, *Sol. Energy Mater.* **3**, 447 (1980).
²C. R. Wronski and D. E. Carlson, *Solid State Commun.* **23**, 421 (1977).
³C. R. Wronski, B. Abeles, G. D. Cody, and T. Tiedje, *Appl. Phys. Lett.* **37**, 96 (1980).
⁴M. J. Thompson, N. M. Johnson, R. J. Nemanich, and C. C. Tsai, *Appl. Phys. Lett.* **39**, 274 (1981).
⁵A. Madan, P. G. LeComber, and W. E. Spear, *J. Non-Cryst. Solids* **20**, 239 (1976).
⁶M. Hirose, T. Suzuki, and G. H. Dohler, *Appl. Phys. Lett.* **34**, 234 (1979); R. Weissfield, P. Viktorovitch, D. Anderson, and W. Paul, *ibid.* **39**, 263 (1981).
⁷J. D. Cohen, D. V. Lang, and J. P. Harbison, *Phys. Rev. Lett.* **45**, 197 (1980).
⁸T. Datta and M. Silver, *Appl. Phys. Lett.* **38**, 903 (1981).
⁹W. E. Spear, R. A. Gibson, D. Yang, P. G. LeComber, G. Muller, and S. Kalbitzer, *J. Phys. (Paris) Colloq.* **42**, C4-1143 (1981).
¹⁰R. A. Street, J. C. Knights, and D. K. Biegelsen, *Phys. Rev. B* **18**, 1880 (1978).
¹¹J. Mort, A. Troup, M. Morgan, S. Grammatica, J. C. Knights, and R. Lujan, *Appl. Phys. Lett.* **38**, 277 (1981).
¹²T. Tiedje, J. M. Cebulka, D. L. Morel, and B. Abeles, *Phys. Rev. Lett.* **46**, 1425 (1981).
¹³R. Weissfield, P. Viktorovich, D. A. Anderson, and W. Paul, *Appl. Phys. Lett.* **39**, 263 (1981).
¹⁴T. Datta and M. Silver, *Solid State Commun.* **38**, 1067 (1981).
¹⁵R. A. Street, *Appl. Phys. Lett.* **41**, 1060 (1982).